JOURNAL OF GUIDANCE, CONTROL, AND DYNAMICS
Vol. 37, No. 6, November–December 2014

Nonlinear Adaptive Output Feedback Control of Flexible-Joint Space Manipulators with Joint Stiffness Uncertainties

Steve Ulrich* and Jurek Z. Sasiadek†
Carleton University, Ottawa, Ontario K1S 5B6, Canada
and
Itzhak Barkana‡
Barkana Consulting, 47209 Ramat-Hasharon, Israel

DOI: 10.2514/1.G000197

Growing research interest in space robotic systems capable of accurately performing autonomous manipulation tasks within an acceptable execution time has led to an increased demand for lightweight materials and mechanisms. As a result, joint flexibility effects become important and represent the main limitation to achieving satisfactory trajectory-tracking performance. This paper addresses the nonlinear adaptive output feedback control problem for flexible-joint space manipulators. Composite control schemes in which decentralized simple adaptive control-based adaptation mechanisms to control the quasi-steady-state robot model are added to a linear correction term to stabilize the boundary-layer model are proposed. An almost strictly passivity-based approach is adopted to guarantee closed-loop stability of the quasi-steady-state model. Simulation results are included to highlight the performance and robustness of the proposed adaptive composite control methodologies to parametric and dynamics modeling uncertainties.

I. Introduction

UPCOMING space robot manipulators, such as the Next-Generation Canadarm developed jointly by MacDonald Detwiler and Associates and the Canadian Space Agency, are expected to be built of slender aluminum-composite links, for which the structural flexibility will be greater than that of their predecessors. Moreover, the latest generation of advanced space robots specifically designed for on-orbit servicing operations are equipped with extremely lightweight joint mechanisms, including harmonic drives. These gear mechanisms have received increasing attention in robotic applications due to their attractive properties, such as high reduction ratio, compact size, low weight, and coaxial assembly. However, with harmonic drives, elastic vibrations of the flexspline are the main issue that significantly challenges control system development. As explained by Sweet and Good [1], revolute joint robot manipulators actuated by dc motors with harmonic drive transmission have relatively large joint stiffness in comparison to other parameters in the system. At the same time, the joint damping is small. This can lead to strongly resonant behavior using rigid control schemes unless the control bandwidth is severely restricted. In addition, when handling large payloads, joint or structural flexibility effects become even more important and can result in significant dynamic interactions. Although both joint and link flexibility effects are important for space manipulators, joint flexibility is often considered more important than link flexibility, at least in the operational range of space robot manipulators [2].

Despite the considerable research work that has been done on the dynamics and control of flexible-joint robot manipulators, the topic remains an important area of contemporary research, and several constraints and limitations are yet to be overcome. Specifically, the most recent studies in this area are mainly focused on addressing the flexible-joint control problem under parametric uncertainties and/or dynamics modeling errors [3–6]. Indeed, earlier flexible-joint control strategies reported in the literature (e.g., nonlinear backstepping control [7], feedback linearization [8], optimal control [9], and robust control [10]) are model-based techniques, and they have reasonably good tracking performance only when substantial knowledge of the plant mathematical model and its parameters are available. Consequently, if significant or unpredictable plant parameter variations arise as a result of joint mechanism degradation, or if there are modeling errors due to complex unmodeled flexible dynamics behaviors, model-based control approaches might perform inadequately.

In this context, this paper considers the adaptive trajectory-tracking problem associated with flexible-joint space manipulators subject to joint stiffness uncertainties and modeling errors. Specifically, the adaptive controller designs proposed in this paper are based on the direct model reference adaptive control idea [11] and deal with modeling errors and parameter uncertainties by time-varying the controllers' gains using computationally efficient adaptation laws, in order to reduce the output tracking errors between an ideal model and the actual robot system.

References [12] and [13] consider direct adaptive composite control of flexible-joint manipulators mounted on a stabilized spacecraft using a simple adaptive control-based gain adaptation mechanism and a fuzzy logic adaptation law, respectively. Although these previous work report satisfactory trajectory-tracking results with good robustness properties to both parametric uncertainties and dynamics modeling errors, no guarantees of closed-loop stability were provided.

The main contribution of this work consists of the development of direct adaptive output feedback approaches that, unlike [12] and [13] and existing indirect composite adaptive controllers for flexible-joint robots (e.g. [14,15]), do not require identification of unknown parameters or mathematical models of the system to be controlled while at the same time guaranteeing closed-loop stability. Specifically, the proposed controllers are composed of a direct adaptive output feedback slow control term that controls the quasi-steady-state model (slow dynamics) and a linear fast control term that controls the boundary-layer model (fast dynamics). Based on recent theoretical developments on stable direct decentralized adaptive control algorithms for nonlinear square systems [16–18], slow control terms employing the decentralized simple adaptive control (DSAC) and the

Presented as Paper 2013-4523 at the AIAA Guidance, Navigation, and Control Conference, Boston, MA, 19–22 August 2013; received 2 August 2013; revision received 26 January 2014; accepted for publication 3 February 2014; published online 9 May 2014.

*Assistant Professor, Department of Mechanical and Aerospace Engineering, 1125 Colonel By Drive. Member AIAA.
†Professor, Department of Mechanical and Aerospace Engineering, 1125 Colonel By Drive. Associate Fellow AIAA.
‡President, 11 Hashomer Street. Associate Fellow AIAA.

decentralized modified simple adaptive control (DMSAC) techniques are proposed. These two design approaches use the almost strictly passive (ASP) conditions for nonlinear systems [19] to guarantee closed-loop convergence of the slow output feedback adaptive control term. Invoking Tychonov's theorem [20], both composite controllers ensure that the tracking errors do not deviate more than of the order $\mathcal{O}(\varepsilon)$ from the quasi-steady state on a finite time interval, where ε is a small positive scalar that is inversely proportional to the joint stiffness matrix.

After reviewing flexible-joint space manipulator dynamics and kinematics, the control problem is presented and an overview of the composite adaptive output feedback control designs is given. Then, preliminary definitions and a theorem that defines under which conditions nonlinear square systems are ASP is reported. Based on these definitions and the ASP theorem, the details of the adaptation mechanisms are discussed, including the proof that the quasi-steady-state model of a flexible-joint robot manipulator with an end-effector Cartesian scaled-position-plus-velocity output feedback is ASP. Finally, numerical examples and closing remarks are given.

II. Robot Dynamics and Kinematics

In this section, the dynamics model of a n-link flexible-joint manipulator is presented using the Euler- Lagrange formulation and then, the kinematics equations specifically applicable to a two-link manipulator are presented.

A. n-Link Flexible-Joint Dynamics

The nonlinear dynamics is derived in terms of kinetic and potential energies stored in the system by the Euler–Lagrange formulation. Since the timescale of robotic motions is assumed to be relatively small compared to the orbital period, orbital mechanics effects are neglected. Also, for space-based robots, microgravitational effects are very small compared to control input forces, and hence can be neglected. As a result, the potential energy is only due to joint elastic effects. By assuming lumped flexibility at the joints, links can be considered rigid and the kinetic energy of the system is obtained as the summation of the kinetic energy of the links (rigid kinetic energy) and of the kinetic energy of the rotors (elastic kinetic energy). Furthermore, each joint can be modeled as a linear torsional spring of constant stiffness. Therefore, under the realistic assumption that the joint damping is small and the joint stiffness is large relatively to the other parameters in the system, the Euler–Lagrange dynamics equations of motion of an n-degree-of-freedom flexible-joint space manipulator mounted on a stabilized spacecraft and actuated by dc motors with harmonic drive transmission are given by [21]

$$M(q)\ddot{q} + C(q,\dot{q})\dot{q} - k(q_m - q) = 0 \tag{1}$$

$$J_m\ddot{q}_m + k(q_m - q) = \tau \tag{2}$$

where $M(q) \in \mathbb{R}^{n\times n}$ denotes the positive-definite link inertia matrix, $C(q,\dot{q}) \in \mathbb{R}^{n\times n}$ represents the centrifugal-Coriolis matrix, $q \in \mathbb{R}^n$ is the link angles, $q_m \in \mathbb{R}^n$ is the motor angles, $J_m \in \mathbb{R}^{n\times n}$ denotes the positive-definite motor inertia matrix, $k \in \mathbb{R}^{n\times n}$ is the joint stiffness matrix, and $\tau \in \mathbb{R}^n$ denotes the control torque vector that will be distributed between a slow control torque τ_s and a fast control torque τ_f, as detailed in Sec. IV. In this dynamics model, the link dynamics [Eq. (1)] and actuator dynamics [Eq. (2)] are only coupled by the elastic torque term $k(q_m - q)$.

B. Two-Link Flexible-Joint Kinematics

For a two-link manipulator, the definition of $M(q)$, $C(q,\dot{q}) \in \mathbb{R}^{2\times 2}$ can be found in [22]. In the following, it is assumed that the two-link robot manipulator system is fully actuated and nonredundant, and that the Jacobian matrix denoted by $J(q) \in \mathbb{R}^{2\times 2}$ has a full rank column. Thus, holonomic constraints can be selected in order for the actual end-effector Cartesian velocity vector, denoted as $\dot{x}_r \in \mathbb{R}^2$ to satisfy the relation

$$\dot{x}_r = J(q)\dot{q} \tag{3}$$

Similarly, it is assumed that there exists a mapping, allowing the end-effector Cartesian position vector, denoted as $x_r \in \mathbb{R}^2$ and defined with respect to the robot reference frame along both axes to be obtained as

$$x_r = \Omega(q) \tag{4}$$

where $\Omega(q) \in \mathbb{R}^2$ is the nonlinear forward kinematics transforming the link positions into end-effector Cartesian position. Assuming that the robot manipulator is equipped with joint encoders and tachometers, Eqs. (3) and (4) can be combined to map joint-space variables into a task-space (Cartesian) vector through the nonlinear transformation [22]

$$\begin{bmatrix} x_r \\ \dot{x}_r \end{bmatrix} = \begin{bmatrix} l_1\cos(q_1) + l_2\cos(q_1+q_2) \\ l_1\sin(q_1) + l_2\sin(q_1+q_2) \\ -l_1\sin(q_1)\dot{q}_1 - l_2\sin(q_1+q_2)(\dot{q}_1+\dot{q}_2) \\ l_1\cos(q_1)\dot{q}_1 + l_2\cos(q_1+q_2)(\dot{q}_1+\dot{q}_2) \end{bmatrix} \tag{5}$$

The scaled-position-plus-velocity output vector of the robot manipulator, denoted as $y \in \mathbb{R}^2$, is then formed as

$$y = \alpha x_r + \dot{x}_r \tag{6}$$

where $\alpha \in \mathbb{R}$ is a known positive-definite scaling gain.

III. Control Objective

The control objective consists of ensuring that the output of the nonlinear flexible-joint manipulator system tracks the output vector $y_m(t)$ of a (not necessarily square) ideal model

$$\dot{x}_m(t) = A_m x_m(t) + B_m u_m(t) \tag{7a}$$

$$y_m(t) = C_m x_m(t) \tag{7b}$$

where

$$x_m = \begin{bmatrix} x_{m_1} \\ \vdots \\ x_{m_{n_m}} \end{bmatrix} \in \mathbb{R}^{n_m}, \quad u_m = \begin{bmatrix} u_{m_1} \\ \vdots \\ u_{m_{p_m}} \end{bmatrix} \in \mathbb{R}^{p_m}, \quad y_m = \begin{bmatrix} y_{m_1} \\ \vdots \\ y_{m_m} \end{bmatrix} \in \mathbb{R}^m$$

are the ideal model states, inputs, and outputs, respectively; and A_m, B_m, and C_m are appropriately dimensioned real matrices. This ideal model represents a realistic description of the desired input–output response that one can expect from the plant under nominal conditions, without requiring any precise knowledge of the actual plant physical parameters. In addition, unlike standard state-feedback model reference adaptive control approaches [23,24], the order of the ideal model does not need to match the order of the plant. For example, the ideal model may be designed as a first- or second-order dynamics model that provides the desired output in response to the user commands. The only restriction on this ideal model is that one must select both n_m and p_m as multiples of the number of output signals, denoted by m. In other words, $n_m = km$ and $p_m = lm$, where k, $l \in \mathbb{N}$ are positive integers. To quantify the control objective, an output error, denoted by $e_y(t) \in \mathbb{R}^m$, is defined as

$$e_y \triangleq y_m - y \tag{8}$$

When the system tracks the ideal model perfectly, i.e., $y_m = y^* = Cx^*$, it moves along some bounded "ideal" state trajectory denoted as $x^*(t) \in \mathbb{R}^n$, where C denotes the output matrix of the system to be controlled. In other words, the ideal plant

$$\dot{x}^* = A^*x^* + B^*u^* \tag{9}$$

moves along x^*, where $A^* \equiv A(x^*, t)$ and $B^* \equiv B(x^*, t)$, and where u^* denotes the ideal control input (to be defined in Sec. V).

To facilitate the subsequent analysis, a state error, denoted by $e_x(t) \in \mathbb{R}^n$, is defined as

$$e_x \triangleq x^* - x \tag{10}$$

Thus, Eq. (8) can be rewritten as

$$e_y = Cx^* - Cx = Ce_x \tag{11}$$

IV. Composite Control Strategies

Following common flexible-joint controller design practice, the singular perturbation-based theory [25] is employed to provide a framework for the design of composite controllers, in which the motor torque control input τ is composed of a slow control term τ_s and a fast control term τ_f

$$\tau = \tau_s + \tau_f \tag{12}$$

where subscript s stands for slow variables defined in the slow timescale t, and the subscript f stands for variables defined in the fast timescale t'. The slow control term is designed to stabilize the quasi-steady-state model (slow dynamics model), whereas the fast-control torque is applied to the boundary-layer model (fast dynamics model).

By defining the joint stiffness matrix of a two-link flexible-joint manipulator as $k = k_1/\varepsilon^2$, with $k_1 \in \mathbb{R}^{2\times2}$ and with $\varepsilon \in \mathbb{R}$ as a small positive parameter, the quasi-steady-state model can obtained with $\varepsilon \to 0$, i.e., with infinitely large joint stiffness. This is equivalent to assuming that the transients due to the fast modes are instantaneous. The resulting quasi-steady-state model has a form equivalent to the rigid-joint dynamics model, and it is given by [26]

$$H(q_s)\ddot{q}_s + C(q_s, \dot{q}_s)\dot{q}_s = \tau_s \tag{13}$$

where

$$H(q_s) \equiv M(q_s) + J_m \tag{14}$$

Let $L \in \mathbb{R}^2$ denote the control torque transmitted through the flexible joints as

$$L = k(q_m - q) = \frac{k_1}{\varepsilon^2}(q_m - q) \tag{15}$$

such that the boundary-layer model can be expressed as [26]

$$\frac{\mathrm{d}^2\eta}{\mathrm{d}t'^2} = k_1\{J_m^{-1}\tau_f - [J_m^{-1} + M^{-1}(q)]\eta\} \tag{16}$$

with $\eta = L - L_s$. To guarantee bounded stability of the entire flexible system, Tychonov's theorem [20], given next, is used.

Theorem 4.1: If the closed-loop quasi-steady-state model has a unique solution q_s defined on the interval $t \in [0, t_1]$, and if the closed-loop boundary-layer model is exponentially stable uniformly in (t, q_s), then there exist ε^* such that $\forall\ \varepsilon \in [0, \varepsilon^*]$, the solution $\{L, q\}$ of the exact system, satisfies

$$L = L_s + \eta + \mathcal{O}(\varepsilon) \tag{17}$$

$$q = q_s + \mathcal{O}(\varepsilon) \tag{18}$$

Similar conclusions are applicable to $\dot{L}$ and $\dot{q}$.

Proof: See [20]. □

To clarify the aforementioned theorem, the composite control objective consists of designing 1) a fast control term that guarantees the exponential stability of the closed-loop boundary-layer model, and 2) a slow control term that guarantees convergence of the tracking error for the closed-loop quasi-steady-state model [27]. This ensures that the tracking error will not deviate more than of the order $\mathcal{O}(\varepsilon)$ from its quasi-steady state on a finite time interval. Thus, the smaller ε is, the greater the tracking accuracy. Recalling the previously given definition of k, it can then be concluded that better tracking results are achieved when the joint stiffness matrix k is greater; in other words, when the boundary-layer model is considerably faster than the quasi-steady-state model. Note that the aforementioned Tychonov's theorem holds only for a finite time interval. Although an extension of this theorem to the infinite time interval [20] does exist, and may be applied in an attempt to show asymptotic stability for sufficiently small ε, it requires exponential stability of the quasi-steady-state model.

A. Boundary-Layer Control Law

Recalling that the boundary-layer model is linear time-invariant, a simple linear correction of the form

$$\tau_f = K_v(\dot{q} - \dot{q}_m) \tag{19}$$

is sufficient to ensure exponential stability of the boundary-layer model [26], where $K_v \in \mathbb{R}^{2\times2}$ is a constant diagonal control gain that provides additional damping of the elastic vibrations at the joints.

B. Quasi-Steady-State Control Laws

As discussed previously, the quasi-steady-state model is equivalent to the rigid-joint dynamics model and is obtained with $\varepsilon \to 0$, i.e., with infinitely large joint stiffness. Two control laws are herein proposed to control this model, and both make use of the transpose of the Jacobian matrix to convert a control force into a control torque as follows:

$$\tau_s = J^T(q)u \tag{20}$$

where $u \in \mathbb{R}^2$ denotes the control input force, herein calculated upon the simple adaptive control (SAC) theory [28] and, respectively, given by

$$u = K_e(t)e_y + K_x(t)x_m + K_u(t)u_m \tag{21}$$

and

$$u = K_e(t)e_y \tag{22}$$

for the DSAC and DMSAC strategies, respectively. As will be shown in Sec. V, the quasi-steady-state model with a scaled-position-plus-velocity output does satisfy the ASP properties, which are necessary to demonstrate the stability of the closed-loop quasi-steady-state model, thereby satisfying Tychonov's theorem.

C. Composite Control Laws

Combining both Eqs. (21) and (22) with Eq. (19), and making use of Eq. (20), results in the DSAC- and DMSAC-based composite control laws, respectively, given by

$$\tau = J^T(q)[K_e(t)e_y + K_x(t)x_m + K_u(t)u_m] + K_v(\dot{q} - \dot{q}_m) \tag{23}$$

$$\tau = J^T(q)K_e(t)e_y + K_v(\dot{q} - \dot{q}_m) \tag{24}$$

The resulting control strategy block diagrams are provided in Figs. 1 and 2.

V. Adaptive Output Feedback Control of the Quasi-Steady-State Model

This section first reviews the conditions under which nonlinear systems are almost strictly passive and presents a theorem that ensures that the quasi-steady-state model of a flexible-joint manipulator with a scaled-position-plus-velocity output matrix is ASP. Then,

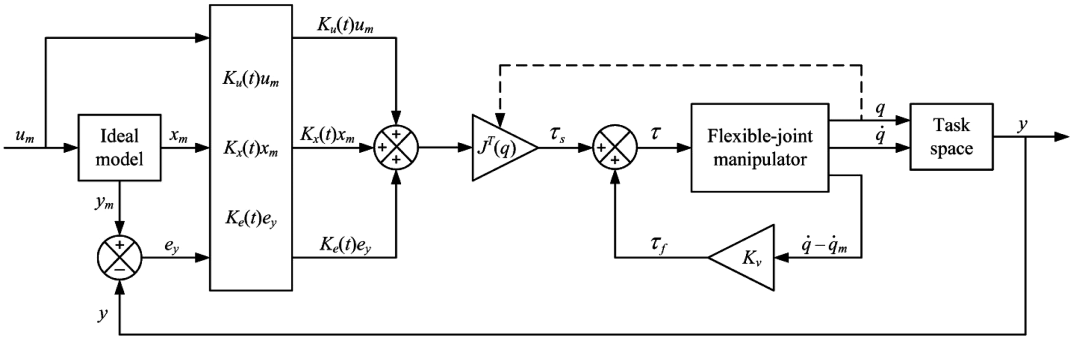

Fig. 1 Block diagram representation of the DSAC-based composite controller.

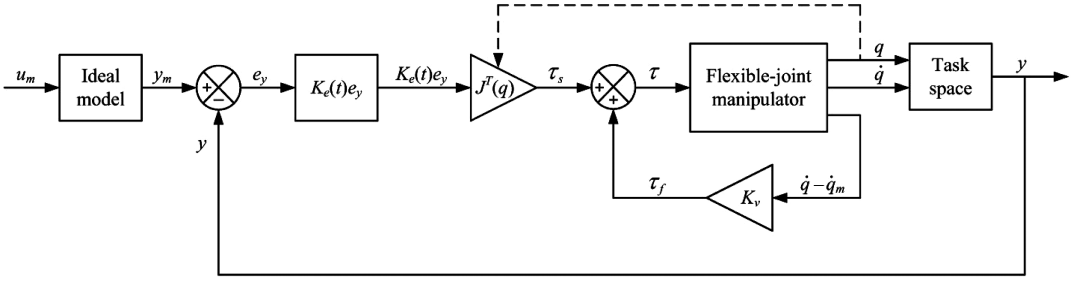

Fig. 2 Block diagram representation of the DMSAC-based composite controller.

two direct adaptive control laws for this ASP model are developed, and finally, the stability analysis of the resulting closed-loop subsystems is discussed.

A. Almost Strictly Passive Nonlinear Systems

Consider a class of nonlinear square systems described by the following state-space transformation formulation:

$$\dot{x}(t) = A(x,t)x(t) + B(x,t)u(t) \tag{25a}$$

$$y(t) = Cx(t) \tag{25b}$$

where

$$x(t) = \begin{bmatrix} x_1 \\ \vdots \\ x_n \end{bmatrix} \in \mathbb{R}^n, \quad u(t) = \begin{bmatrix} u_1 \\ \vdots \\ u_m \end{bmatrix} \in \mathbb{R}^m, \quad y(t) = \begin{bmatrix} y_1 \\ \vdots \\ y_m \end{bmatrix} \in \mathbb{R}^m$$

are the system states, inputs, and outputs, respectively; and $A(x,t)$, $B(x,t)$, and C are appropriately dimensioned real matrices.

Definition 5.1: The nonlinear system described by Eq. (25) is uniformly strictly minimum phase if its zero dynamics is uniformly stable. In other words, there exist two matrices $M(x,t)$ and $N(x,t)$ satisfying the following relations:

$$CM = 0 \tag{26a}$$

$$NB(x,t) = 0 \tag{26b}$$

$$NM = I_{n-m} \tag{26c}$$

such that the resulting zero dynamics given by

$$\dot{z}(t) = A_z(x,t)z(t) \tag{27}$$

is uniformly asymptotically stable. In Eq. (27), $A_z(x,t)$ denotes the system matrix of the zero dynamics and is equal to

$$(\dot{N}(x,t) + N(x,t)A(x,t))M(x,t)$$

In Eq. (26c), I_{n-m} denotes the $(n-m)\times(n-m)$ identity matrix.

Definition 5.2: The nonlinear system described by Eq. (25) is ASP if there exist two positive definite symmetric (PDS) matrices $P(x,t)$ and $Q(x,t)$ and a constant output feedback gain $\tilde{K}_e$ such that the closed-loop system

$$\dot{x}(t) = \left[A(x,t) - B(x,t)\tilde{K}_e C\right]x(t) \tag{28}$$

simultaneously satisfies the following ASP relations:

$$\dot{P}(x,t) + P(x,t)[A(x,t) - B(x,t)\tilde{K}_e C] + \left[A(x,t) - B(x,t)\tilde{K}_e C\right]^T P(x,t) = -Q(x,t) \tag{29a}$$

$$P(x,t)B(x,t) = C^T \tag{29b}$$

Lyapunov differential equation (29a) shows that the closed-loop system is uniformly asymptotically stable, whereas second relation equation (29b) implies that the product $CB(x,t)$ is a PDS.

Theorem 5.1: Any nonlinear systems described by Eq. (25), which is uniformly strictly minimum phase and with the product $CB(x,t)$ being PDS, is ASP.

Proof: See [16]. □

B. Almost Strict Passivity of the Quasi-Steady-State Model

Let us rewrite the joint-space dynamics of the quasi-steady-state model defined by Eq. (13) into the task-space dynamics as follows:

$$\Lambda(q_s)\ddot{x}_{r_s} + \Pi(q_s,\dot{q}_s)\dot{x}_{r_s} = u \tag{30}$$

where $\Lambda(q_s)$, $\Pi(q_s,\dot{q}_s) \in \mathbb{R}^{2\times 2}$ denote the pseudoinertia and Coriolis/centrifugal matrices, respectively, given by

$$\Lambda(q_s) = J^{-T}(q_s)M(q_s)J^{-1}(q_s) \tag{31a}$$

$$\Pi(q_s,\dot{q}_s) = J^{-T}(q_s)C(q_s,\dot{q}_s)J^{-1}(q_s) + \Lambda(q_s)J(q_s)\dot{J}^{-1}(q_s) \quad (31b)$$

$$u = J^{-T}(q)\tau_s \quad (31c)$$

Theorem 5.2: The quasi-steady-state model of a two-link flexible-joint manipulator expressed in the task-space by Eq. (30) with a scaled-position-plus-velocity output matrix is ASP.

Proof: The nonlinear system dynamics can be expressed in a standard state-space representation, with matrices given by

$$A = \begin{bmatrix} 0 & I_2 \\ 0 & -\Lambda^{-1}(q_s)\Pi(q_s,\dot{q}_s) \end{bmatrix} \quad B = \begin{bmatrix} 0 \\ \Lambda^{-1}(q_s) \end{bmatrix} \quad C = \begin{bmatrix} \alpha I_2 & I_2 \end{bmatrix}$$

where the state vector $[\,x_{r_s} \quad \dot{x}_{r_s}\,]^T$ corresponds to Eq. (5) evaluated in the slow timescale, i.e., at q_s and $\dot{q}_s$. Thus, is can be seen that the product of the output and input system matrices is PDS:

$$CB = [\,\alpha I_2 \quad I_2\,]\begin{bmatrix} 0 \\ \Lambda^{-1}(q_s) \end{bmatrix} = \Lambda^{-1}(\dot{q_s}) > 0 \quad (32)$$

Moreover, noting that the matrices $M(x,t)$ and $N(x,t)$ can also be selected as being constant, a simple selection that satisfies Eq. (26) is

$$M = \begin{bmatrix} I_2 \\ -\alpha I_2 \end{bmatrix} \qquad N = \begin{bmatrix} I_2 & 0 \end{bmatrix} \quad (33)$$

The system matrix of the zero dynamics, A_z, is therefore given by

$$A_z = NAM = -\alpha I_2 \quad (34)$$

The zero dynamics equation is thus of the form

$$\dot{z} = A_z z = -\alpha z \quad (35)$$

which shows that the zero dynamics is stable and that the nonlinear dynamics of the quasi-steady-state model is uniformly minimum-phase. Invoking Theorem 5.1 completes the proof. □

A similar proof can be obtained for a rigid-joint manipulator dynamics model expressed in the joint space, as shown in [19]. Note that, although the aforementioned development was presented for a two-link manipulator for simplicity purposes, the proof previously presented might be extended for an n-link manipulator, as long as it is modeled as a square system.

C. Adaptive Control Laws

Given that the quasi-steady-state model of a flexible-joint manipulator that employs a scaled-position-plus-velocity feedback is ASP, stability of the quasi-steady-state model can be guaranteed by using either the decentralized simple adaptive control or the decentralized modified simple adaptive control techniques [16–18]. These techniques are called "decentralized" since only the diagonal elements of each adaptation gain matrix are considered in the adaptation laws. This is the main difference between the standard SAC approach and the decentralized ones. By omitting the cross couplings, each axis is controlled separately and independently, which make the decentralized approaches better suited for real-time applications with low computational power.

1. Decentralized Simple Adaptive Control

The standard SAC algorithm given by Eq. (21) is adopted as the slow control term, where $K_e(t) \in \mathbb{R}^{m\times m}$ is the time-varying stabilizing control gain matrix, and $K_x(t) \in \mathbb{R}^{m\times m_n}$ and $K_u(t) \in \mathbb{R}^{m\times p_m}$ are time-varying feedforward control gain matrices that contribute to bringing the output tracking error to zero.

Each control gain matrix is calculated as the summation of a proportional and an integral component as follows:

$$K_e(t) = K_{Pe}(t) + K_{Ie}(t) \quad (36)$$

$$K_x(t) = K_{Px}(t) + K_{Ix}(t) \quad (37)$$

$$K_u(t) = K_{Pu}(t) + K_{Iu}(t) \quad (38)$$

where only the integral adaptive control terms are absolutely necessary to guarantee the stability of the direct adaptive control system. However, including the proportional adaptive control terms increases the rate of convergence of the adaptive system toward perfect tracking.

Using the DSAC adaptation mechanism [16–18], the proportional and the integral components of the stabilizing control gain in Eq. (36), $K_{Pe}(t), K_{Ie}(t) \in \mathbb{R}^{m\times m}$, are both updated by the output tracking error only, which results in the following adaptation law:

$$K_{Pe}(t) = \text{diag}\{e_y e_y^T\}\Gamma_{Pe} \quad (39a)$$

$$\dot{K}_{Ie}(t) = \text{diag}\{e_y e_y^T\}\Gamma_{Ie} \quad (39b)$$

The components of the feedforward gain matrices $K_{Px}(t)$, $K_{Ix}(t) \in \mathbb{R}^{m\times n_m}$, and $K_{Pu}(t)$, $K_{Iu}(t) \in \mathbb{R}^{m\times n_m}$ are updated in a similar fashion as follows:

$$K_{Px}(t) = R^T\text{diag}\{Re_y x_m^T\}\Gamma_{Px} \quad (40a)$$

$$\dot{K}_{Ix}(t) = R^T\text{diag}\left\{Re_y x_m^T\right\}\Gamma_{Ix} \quad (40b)$$

$$K_{Pu}(t) = T^T\text{diag}\{Te_y u_m^T\}\Gamma_{Pu} \quad (40c)$$

$$\dot{K}_{Iu}(t) = T^T\text{diag}\{Te_y u_m^T\}\Gamma_{Iu} \quad (40d)$$

where

$$R = \begin{bmatrix} I_m \\ I_m \\ \vdots \\ I_m \end{bmatrix} \in \mathbb{R}^{n_m\times m}, \qquad T = \begin{bmatrix} I_m \\ I_m \\ \vdots \\ I_m \end{bmatrix} \in \mathbb{R}^{p_m\times m}$$

and where Γ_{Pe}, $\Gamma_{Ie} \in \mathbb{R}^{m\times m}$, Γ_{Px}, $\Gamma_{Ix} \in \mathbb{R}^{n_m\times n_m}$, and Γ_{Pu}, $\Gamma_{Iu} \in \mathbb{R}^{p_m\times p_m}$ are constant diagonal matrices that control the rate of adaptation of the algorithm.

The adaptive algorithm can be rewritten in the following concise form:

$$u = K(t)r \quad (41)$$

where $K(t) \in \mathbb{R}^{m\times(m+n_m+p_m)}$ and $r \in \mathbb{R}^{(m+n_m+p_m)}$ are, respectively, defined as

$$K(t) = [\,K_e(t) \quad K_x(t) \quad K_u(t)\,] = K_P(t) + K_I(t) \quad (42)$$

$$r = [\,e_y^T \quad x_m^T \quad u_m^T\,]^T \quad (43)$$

With this representation, $K_P(t), K_I(t) \in \mathbb{R}^{m\times(m\times n_m+p_m)}$ are updated as follows:

$$K_P(t) = S^T\text{diag}\{Se_y r^T\}\Gamma_P \quad (44a)$$

$$\dot{K}_I(t) = S^T \text{diag}\{S e_y r^T\} \Gamma_I \tag{44b}$$

where $\Gamma_P, \Gamma_I \in \mathbb{R}^{(m+n_m+p_m)\times(m+n_m+p_m)}$, and where the scaling matrix S is given by

$$S = \begin{bmatrix} I_m \\ I_m \\ \vdots \\ I_m \end{bmatrix} \in \mathbb{R}^{(m+n_m+p_m)\times m}$$

Time-differentiating Eq. (10), after some algebra, gives the following differential equation of the state error:

$$\dot{e}_x = (A - B\tilde{K}_e C)e_x + (A^* - A)x^* + (B^* - B)u^* - BK_P(t)r - B(K_I(t) - \tilde{K})r \tag{45}$$

where $\tilde{K}_e \in \mathbb{R}^{m\times m}$ is any constant stabilizing control gain, and where $\tilde{K} \in {}^{m\times(m+n_m+p_m)}$ is defined as

$$\tilde{K} = [\,\tilde{K}_e \quad \tilde{K}_x \quad \tilde{K}_u\,] \tag{46}$$

with $\tilde{K}_x \in \mathbb{R}^{m\times n_m}$ and $\tilde{K}_u \in \mathbb{R}^{m\times p_m}$ denoting the constant ideal feedforward control gains. When the control is such that perfect tracking occurs, the output tracking error is

$$e_y = y_m - y = 0 \tag{47}$$

In this case, the ideal control input denoted by $u^* \in \mathbb{R}^m$ is given by

$$u^* = \tilde{K}_x x_m + \tilde{K}_u u_m \tag{48}$$

2. Decentralized Modified Simple Adaptive Control

To decrease the computational power required to implement the adaptive control algorithm, the modified SAC (MSAC) idea can be used. With MSAC, as opposed to SAC, the control law is obtained by retaining only the error-related adaptive control gain $K_e(t)$ in the algorithm. The name "modified SAC" is employed here to distinguish the algorithm from the usual SAC algorithm that employs the feedforward terms. Note that neglecting the feedforward terms is not a new idea, since it was first proposed by Fradkov [29,30]. Later on, Barkana and Kaufman [31] also demonstrated that only the stabilizing control gain matrix $K_e(t)$ was absolutely required for the stability of the adaptive control methodology. More recently, the MSAC approach was successfully applied for the planetary entry on Mars under large atmospheric density uncertainties [32]. Adopting the MSAC approach to compute the slow control torque yields the control law given by Eq. (22), with $K_e(t) = K_{Pe}(t) + K_{Ie}(t)$, where $K_{Pe}(t)$ and $K_{Ie}(t)$ are updated with the decentralized adaptation law given in Eq. (39).

With the resulting DMSAC methodology, the ideal control input u^* is zero, since $e_y = 0$ along the ideal trajectory. In this case, the differential equation of the state error becomes

$$\dot{e}_x = (A - B\tilde{K}_e C)e_x + (A^* - A)x^* - BK_{Pe}(t)e_y - B(K_{Ie}(t) - \tilde{K}_e)e_y \tag{49}$$

D. Brief Review of Stability

To show the asymptotic convergence of the tracking errors, and that the adaptive gains are bounded, the proof of stability must consider the adaptive system defined by both Eqs. (44b) and (45), and Eqs. (39b) and (49), for DSAC and DMSAC, respectively.

1. Decentralized Simple Adaptive Control

Theorem 5.3: When applied to the nonlinear ASP task-space dynamics representation of the quasi-steady-state model defined by Eq. (30), which employs a scaled-position-plus-velocity output feedback, and under the assumption that the ideal model satisfies $n_m = km$ and $p_m = lm$, the adaptive control law given by Eq. (21) with DSAC adaptation mechanism [Eqs. (36–40)] ensures that all adaptive control gains are bounded under closed-loop operation, and it results in asymptotic convergence of the state and output tracking errors in the sense that

$$\|e_y\| \to 0 \quad \text{and} \quad \|e_x\| \to 0 \quad \text{as } t \to \infty$$

where $\|\bullet\|$ denotes the standard Euclidean norm of a vector.

Proof: Choosing a continuously differentiable positive-definite quadratic Lyapunov function of the form

$$V = e_x^T P e_x + \text{tr}[(K_I(t) - \tilde{K})\Gamma_I^{-1}(K_I(t) - \tilde{K})^T] \tag{50}$$

and using the ASP relations given by Eq. (29) results in the following time derivative of the Lyapunov function:

$$\dot{V} = -e_x^T Q e_x - 2e_x^T C^T S^T \text{diag}\{S C e_x r^T\}\Gamma_P r \tag{51}$$

While the Lyapunov function in Eq. (50) is positive-definite quadratic in terms of all state variables of the dynamical system $\{e_x, K_I(t)\}$, its time derivative given in Eq. (51) only includes the state error e_x, and it is therefore negative definite in e_x and negative semidefinite in the state-gain space $\{e_x, K_I(t)\}$. Stability of the adaptive system is therefore guaranteed from Lyapunov stability theory, and all state errors (and output errors), as well as adaptive control gains, are bounded. Furthermore, LaSalle's invariance principle for non-autonomous systems [19,28,33,34] can be used to demonstrate the asymptotic stability of the tracking errors.

Remark: The well-known σ terms [35] can be included in the gain adaptation mechanisms to ensure that the integral adaptive control gains remain bounded in cases where the tracking error would not reach zero. With this adjustment, the time-varying integral control gains are obtained as follows:

$$\dot{K}_{Ie}(t) = \text{diag}\{e_y e_y^T\}\Gamma_{Ie} - \sigma_e K_{Ie}(t) \tag{52a}$$

$$\dot{K}_{Ix}(t) = R^T(\text{diag}\{R e_y x_m^T\}\Gamma_{Ix} - \text{diag}\{\sigma_x R K_{Ix}(t)\}) \tag{52b}$$

$$\dot{K}_{Iu}(t) = T^T(\text{diag}\{T e_y u_m^T\}\Gamma_{Iu} - \text{diag}\{\sigma_u T K_{Iu}(t)\}) \tag{52c}$$

and similarly,

$$\dot{K}_I(t) = S^T(\text{diag}\{S e_y r_T\}\Gamma_I - \text{diag}\{\sigma_I S K_I(t)\}) \tag{53}$$

where $\sigma_e \in \mathbb{R}^{m\times m}$, $\sigma_x \in \mathbb{R}^{n_m\times n_m}$, $\sigma_u \in \mathbb{R}^{p_m\times p_m}$, and $\sigma_I \in \mathbb{R}^{(m+n_m+p_m)\times(m+n_m+p_m)}$ denote the coefficient matrices. With this modification to the DSAC algorithm, the derivative of the Lyapunov function becomes

$$\dot{V} = -e_x^T Q e_x - 2e_x^T C^T S^T \text{diag}\{S C e_x r^T\}\Gamma_P r - 2\text{tr}[S^T \text{diag}\{\sigma_I S K_I(t)\}\Gamma_I^{-1}(K_I(t) - \tilde{K})^T] \tag{54}$$

Thus, according to the Lyapunov–LaSalle theorem, the application of the DSAC algorithm with the forgetting terms results in bounded error tracking. Note that, although it affects the proof of stability, the use of the DSAC control law with this adjustment is preferable in most practical applications. Without the σ terms, the integral adaptive gains are allowed to increase for as long as there is a tracking error. When the integral gains reach certain values, they have a stabilizing effect on the system and the tracking error begins to decrease. However, if the tracking error does not reach zero for some reason, the integral gains will continue to increase and eventually diverge. On the other hand, with the σ terms, the integral gains increase as required

(e.g., due to large tracking errors), and decrease when large gains are no longer necessary. In fact, with these σ terms, the integral gains are obtained as a first-order filtering of the tracking errors, and they cannot diverge unless the tracking errors diverge. □

2. Decentralized Modified Simple Adaptive Control

Theorem 5.4: When applied to the nonlinear ASP task-space dynamics representation of the quasi-steady-state model defined by Eq. (30), which employs a scaled-position-plus-velocity output feedback, and under the assumption that the ideal model satisfies $n_m = km$ and $p_m = lm$, the adaptive control law given by Eq. (22) with DMSAC adaptation mechanism [Eqs. (36) and (39)] ensures that all adaptive control gains are bounded under closed-loop operation and results in asymptotic convergence of the state and output tracking errors in the sense that

$$\|e_y\| \to 0 \quad \text{and} \quad \|e_x\| \to 0 \quad \text{as } t \to \infty$$

Proof: Choosing a continuously-differentiable positive-definite quadratic Lyapunov function of the form

$$V = e_x^T P e_x + \text{tr}[(K_{Ie}(t) - \tilde{K}_e)\Gamma_{Ie}^{-1}(K_{Ie}(t) - \tilde{K}_e)^T] \tag{55}$$

and using the ASP relations given by Eq. (29) results in the following time derivative of the Lyapunov function:

$$\dot{V} = -e_x^T Q e_x - 2e_x^T C^T \text{diag}\{Ce_x e_x^T C^T\}\Gamma_{Pe} Ce_x \tag{56}$$

Therefore, the same conclusions about stability than those obtained with the DSAC algorithm (see Theorem 5.3) can be drawn.

Remark: By considering σ_e in the algorithm, $\dot{K}_{Ie}(t)$ is obtained with Eq. (52a) and the Lyapunov derivative becomes

$$\begin{aligned}\dot{V} = &-e_x^T Q e_x - 2e_x^T C^T \text{diag}\{Ce_x e_x^T C^T\}\Gamma_{Pe} Ce_x \\ &- 2tr[\sigma_e K_{Ie}(t)\Gamma_{Ie}^{-1}(K_{Ie}(t) - \tilde{K}_e)^T]\end{aligned} \tag{57}$$

and the same conclusions about the impact on stability than those obtained with the DSAC algorithm (see Theorem 5.3) can be drawn. □

VI. Numerical Simulation Results

To validate the nominal trajectory-tracking performance, the control strategies were applied to the linear joint stiffness robot manipulator described in Sec. II. Although Readman [36] suggests joint stiffness values on the order of 10^4 N · m/rad for a harmonic drive joint and 10^3 N · m/rad for a flexible coupling joint, the joint parameters are based on work by Cao and de Silva [15], which is representative of manipulators with obvious flexible effects in their joints. The parameters of the two-link flexible-joint manipulator were thus selected as $l_1 = l_2 = 4.5$ m, $m_1 = m_2 = 1.5075$ kg, $J_{m_1} = J_{m_2} = 1$ kg · m^2, $k_1 = k_2 = 500$ N · m/rad, and $\alpha = 0.5$. In this work, the ideal model was designed to incorporate the desired inpu–output plant behavior, which is expressed in terms of the ideal damping ratio $\zeta \in \mathbb{R}$ and undamped natural frequency $\omega_n \in \mathbb{R}$, as follows:

$$A_m = \begin{bmatrix} 0 & 0 & 1 & 0 \\ 0 & 0 & 0 & 1 \\ -\omega_n^2 & 0 & -2\zeta\omega_n & 0 \\ 0 & -\omega_n^2 & 0 & -2\zeta\omega_n \end{bmatrix},$$

$$B_m = \begin{bmatrix} 0 & 0 & 0 & 0 \\ 0 & 0 & 0 & 0 \\ \omega_n^2 & 0 & 0 & 0 \\ 0 & \omega_n^2 & 0 & 0 \end{bmatrix}, \qquad C_m = [\alpha I_2 \quad I_2]$$

with

$$x_m = \begin{bmatrix} x_{r_m} \\ \dot{x}_{r_m} \end{bmatrix} \in \mathbb{R}^4, \qquad u_m = \begin{bmatrix} x_{r_d} \\ \dot{x}_{r_d} \end{bmatrix} \in \mathbb{R}^4$$

where x_{r_d}, $\dot{x}_{r_d} \in \mathbb{R}^2$ denote the desired Cartesian position and velocity vectors related to the commanded end-effector trajectory. Here, based on previous work in the area of flexible manipulator control [37,38], a 12.6 × 12.6 m trajectory to be tracked in 60 s by the end effector is considered. While such a high-speed trajectory might be difficult to apply practically, it was nevertheless selected because it renders the nonlinearities and flexibility effects significant. In other words, its inherent control difficulties make it a challenging benchmark trajectory, as the instantaneous changes in commanded direction at the corners of the square while the end effector is moving at a high speed are likely to induce joint vibrations. In this context, the control performance consists of providing satisfactory tracking performance along each side of the trajectory while minimizing the end-effector positioning overshoot at each corner, which is defined as the maximum *x*-*y* Cartesian separation distance following each direction change and calculated between the desired square trajectory and the achieved end-effector path.

Aside from the scaling parameter that is assumed to be known, the ideal model is not based on any modeling of the plant and was designed with $\omega_n = 10$ rad/s, $\zeta = 0.9$, and $\alpha = 0.5$. The control parameters of the DSAC composite control algorithm were determined as follows:

$$\Gamma_{Pe} = 15I_2, \quad \Gamma_{Ie} = 50I_2, \quad \Gamma_{Px} = \Gamma_{Pu} = 0.1I_4, \quad \Gamma_{Ix} = \Gamma_{Iu} = 0.2I_4$$

$$\sigma_e = 0.1I_2, \quad \sigma_x = \sigma_u = \text{diag}\{0.9 \;\; 0.9 \;\; 0.4 \;\; 0.4\}, \quad K_v = 120I_2$$

and the control parameters of the DMSAC composite controller were selected as follows:

$$\Gamma_{Pe} = 15I_2, \qquad \Gamma_{Ie} = 35I_2, \qquad \sigma_e = 0.03I_2, \qquad K_v = 35I_2$$

Note that the controllers may be sensitive to the selected control parameters. As a result, different trajectory-tracking performances may be obtained by choosing different parameters than those previously listed. However, as will be demonstrated through the simulation results obtained, once the adaptive algorithms are properly designed under nominal conditions, the results are not very sensitive to uncertainties in the parameters and modeling errors, especially when compared to fixed-gain model-free controllers or indirect adaptive control strategies designed for the same nominal flexible-joint manipulator and validated under the same off-nominal conditions [39].

The integral structure of the adaptive integral gains is computed online using a standard Tustin algorithm, and all integral gains were initialized to zero. The control parameters were selected to provide satisfactory tracking performance along each side of the 12.6 × 12.6-m-square trajectory, with acceptable positioning overshoots at the corners when applied to the two-link flexible-joint robot modeled with the nominal linear joint stiffness dynamics representation described in Sec. II and with physical characteristics previously given. Also, the values of the selected σ terms are relatively small, since they are only to prevent the integral adaptive gains from reaching excessively high values or diverging in time.

Results for the DMSAC and the DSAC control laws are shown in Figs. 3–5 and in Figs. 6–10, respectively. As shown in these figures, while both controllers' trajectories exhibit minimal overshoots at each direction change, with rapid settling to a steady-state along each side of the trajectory, the DSAC composite control strategy provides improved tracking results when compared to the DMSAC composite controller. This is demonstrated in Figs. 3 and 6, where the DMSAC control strategy exhibits greater positioning overshoots; 0.117, 0.112, and 0.104 m, in comparison with 0.082, 0.079, and 0.079 m for the DSAC control law at the first, second, and third direction changes, respectively. The corresponding time-varying control gains, shown in Figs. 5 and 8–10 for each controller, respectively, increase sharply

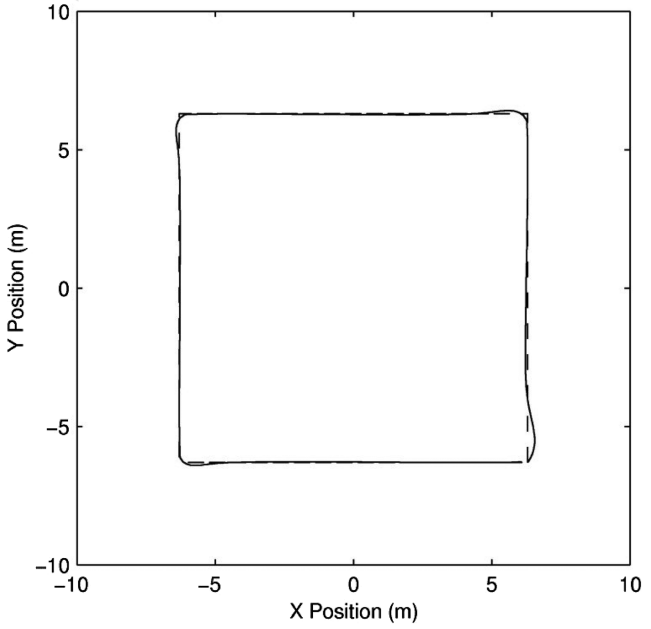

Fig. 3 DMSAC trajectory-tracking results, nominal linear joint stiffness manipulator ($k = 500I_2$ N · m).

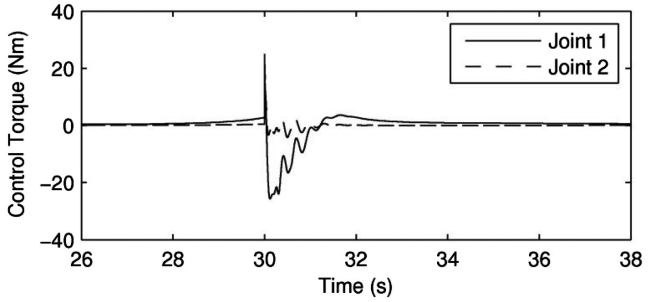

Fig. 4 DMSAC control input torque, nominal linear joint stiffness manipulator ($k = 500I_2$ N · m).

when the end effector reaches each corner of the square trajectory, thus adapting the control laws to reduce tracking errors and positioning overshoots. It is also important to note that, as observed in this Figs. 5 and 8–10, the adaptation rates (i.e., the rates of change of the adaptive gains) at each direction switch are large. These high adaptation rates ensure that the required gains are provided at the correct time, with peaks occurring only at the corners of the square trajectory. In other words, fast adaptation rates allow the controller to use low gains and to increase them only when necessary. Figures 4 and 7 illustrate the control inputs for both controllers. As shown in

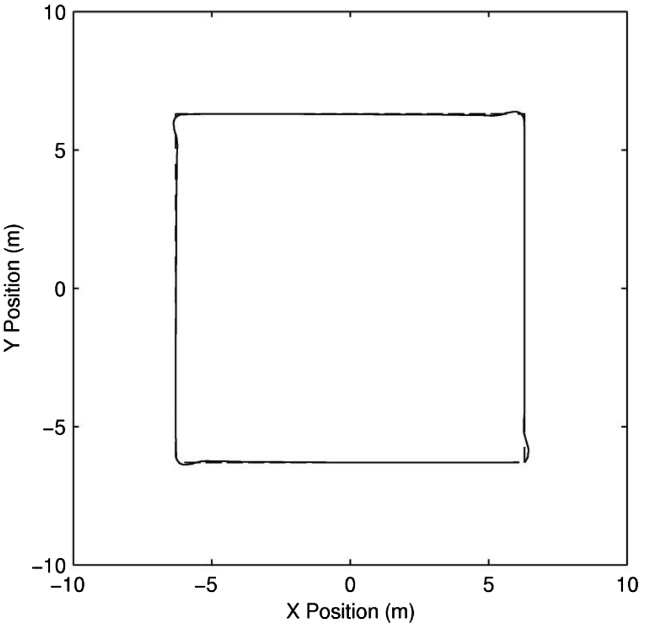

Fig. 6 DSAC trajectory-tracking results, nominal linear joint stiffness manipulator ($k = 500I_2$ N · m).

these figures, larger control input magnitudes are associated with the DSAC strategy, due to the introduction of additional feedforward control terms in the control structure. Indeed, these terms increase the overall control effort, as required to improve the tracking performance.

To validate the robustness to parametric uncertainties, the same DMSAC and DSAC composite controllers tuned for the nominal robot manipulator were applied to the uncertain linear joint stiffness robot model, which is defined by significantly lower joint stiffness coefficients, i.e., with $k_1 = k_2 = 200$ N · m/rad. The results are provided in Figs. 11–18. Both composite control methodologies achieved similar tracking performance in terms of end-effector

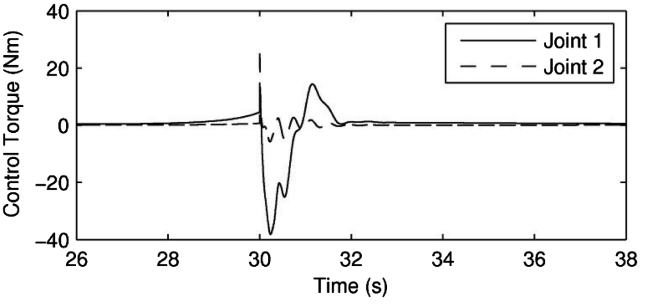

Fig. 7 DSAC control input torque, nominal linear joint stiffness manipulator ($k = 500I_2$ N · m).

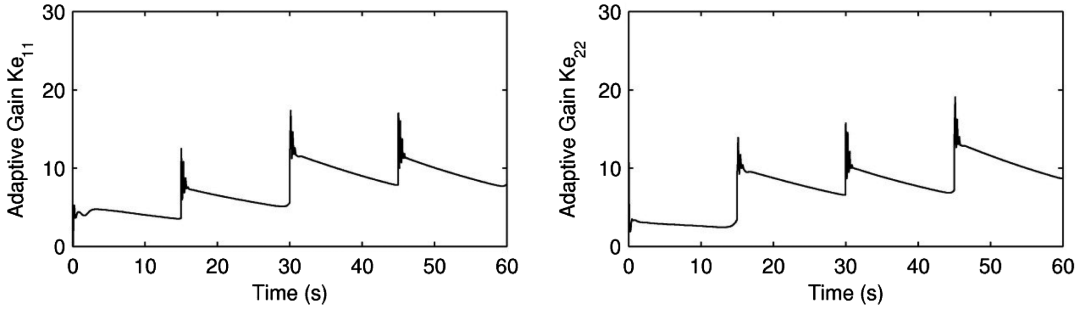

Fig. 5 Adaptation history of the DMSAC composite controller gains K_e, nominal linear joint stiffness manipulator ($k = 500I_2$ N · m).

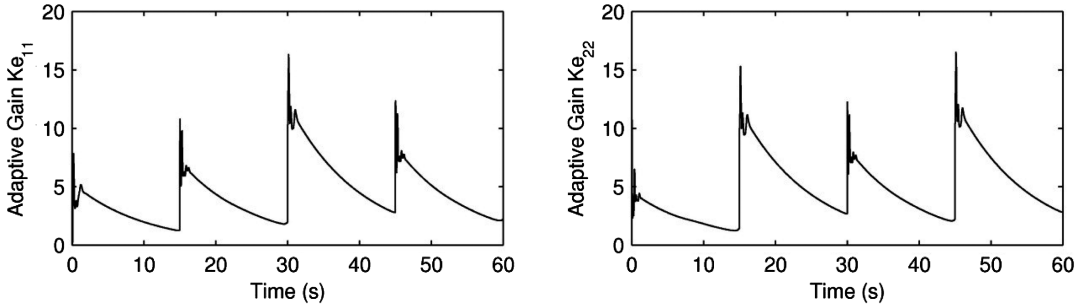

Fig. 8 Adaptation history of the DSAC composite controller gains K_e, nominal linear joint stiffness manipulator ($k = 500I_2$ N · m).

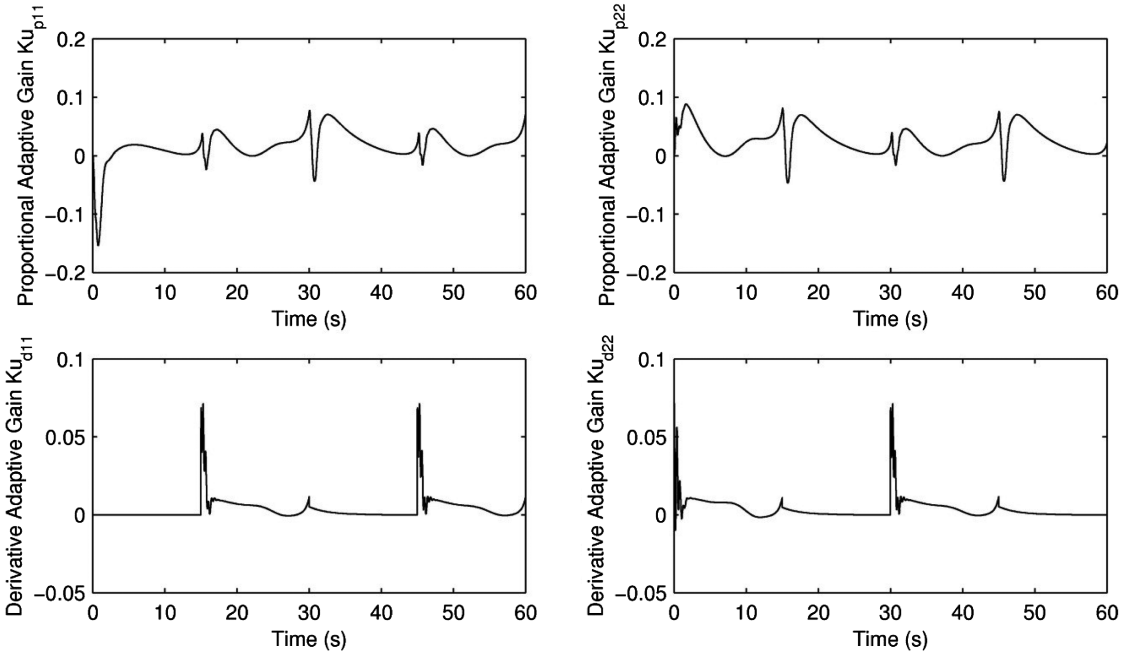

Fig. 9 Adaptation history of the DSAC composite controller gains K_u, nominal linear joint stiffness manipulator ($k = 500I_2$ N · m).

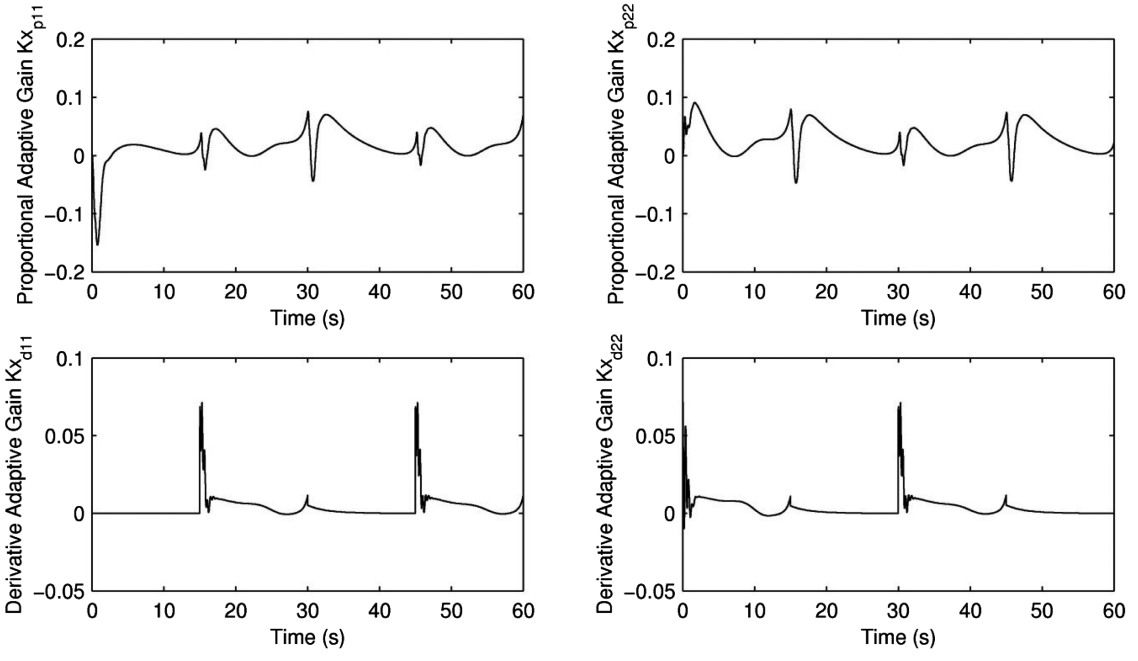

Fig. 10 Adaptation history of the DSAC composite controller gains K_x, nominal linear joint stiffness manipulator ($k = 500I_2$ N · m).

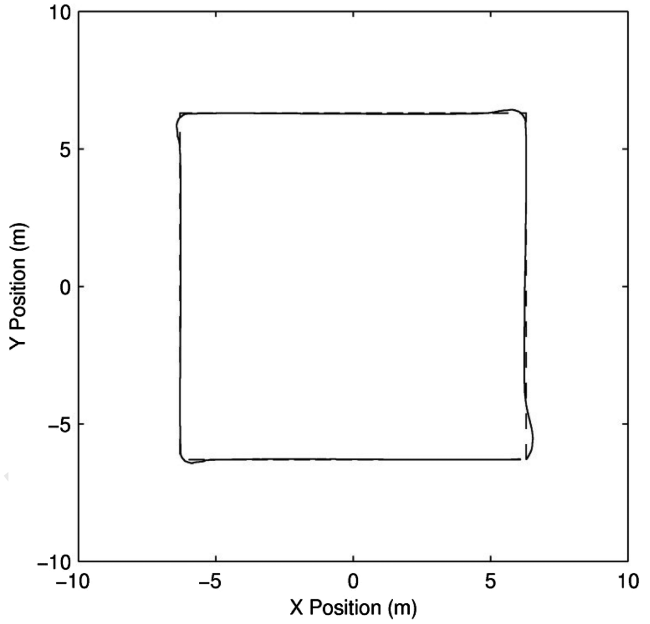

Fig. 11 DMSAC trajectory-tracking results, uncertain linear joint stiffness manipulator ($k = 200I_2$ N · m).

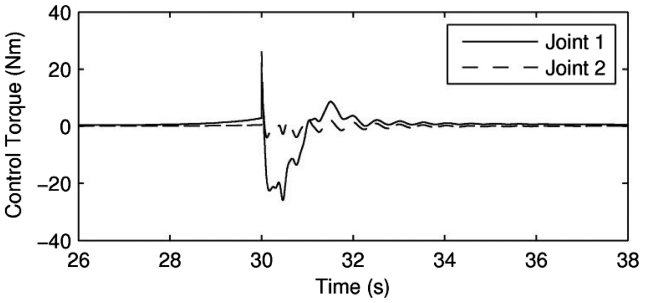

Fig. 12 DMSAC control input torque, uncertain linear joint stiffness manipulator ($k = 200I_2$ N · m).

positioning overshoots: 0.124, 0.126, and 0.121 m for the DMSAC strategy, compared with 0.127, 0.129, and 0.123 m for the DSAC strategy. However, with the DSAC approach, the settling time between two direction changes is larger. This is likely due to the increased oscillations in control inputs associated with the DSAC controller in response to the higher flexibilities in the manipulator system, as illustrated in Fig. 15. Recalling that the Γ parameters control the rate of adaptation of the control gains, this is a direct consequence of the larger Γ parameters selected for this controller. This is observed by very large adaptation rates in the control gains adaptation history (see Figs. 16–18). In turn, this makes the DSAC controller more sensitive to sudden changes in the desired trajectory, which results in increased oscillations and settling times in the end-effector positioning, as demonstrated by the obtained results. Decreasing the Γ parameters would reduce these large adaptation rates, thereby also diminishing the oscillations in the control inputs and end-effector positioning after each direction change.

To validate the performance of the proposed controllers to dynamics modeling errors, both adaptive control schemes were

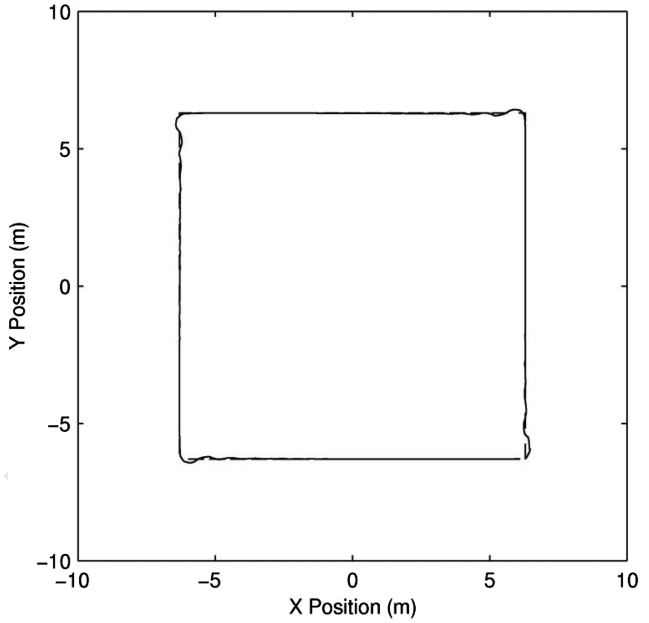

Fig. 14 DSAC trajectory-tracking results, uncertain linear joint stiffness manipulator ($k = 200I_2$ N · m).

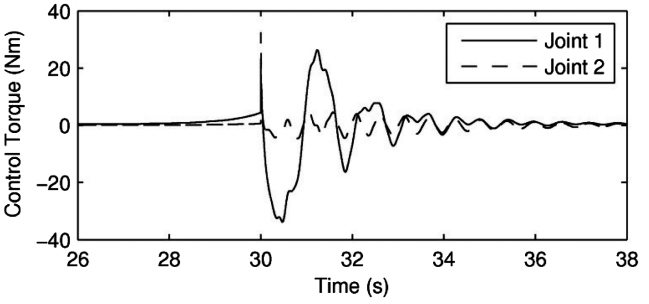

Fig. 15 DSAC control input torque, uncertain linear joint stiffness manipulator ($k = 200I_2$ N · m).

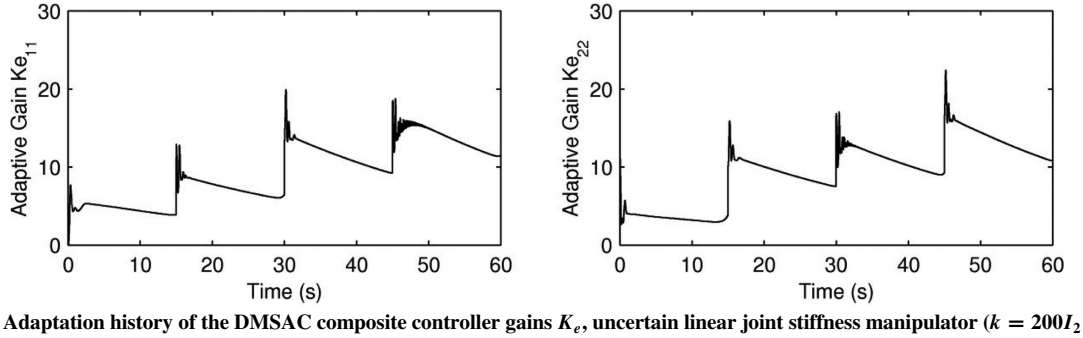

Fig. 13 Adaptation history of the DMSAC composite controller gains K_e, uncertain linear joint stiffness manipulator ($k = 200I_2$ N · m).

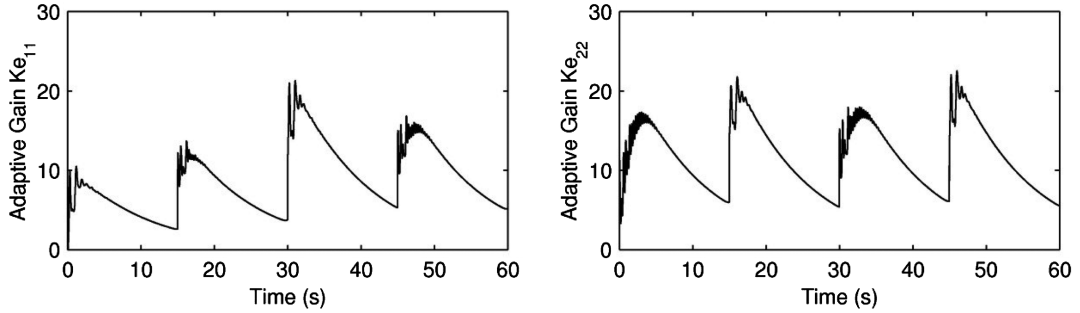

Fig. 16 Adaptation history of the DSAC composite controller gains K_e, uncertain linear joint stiffness manipulator ($k = 200I_2$ N · m).

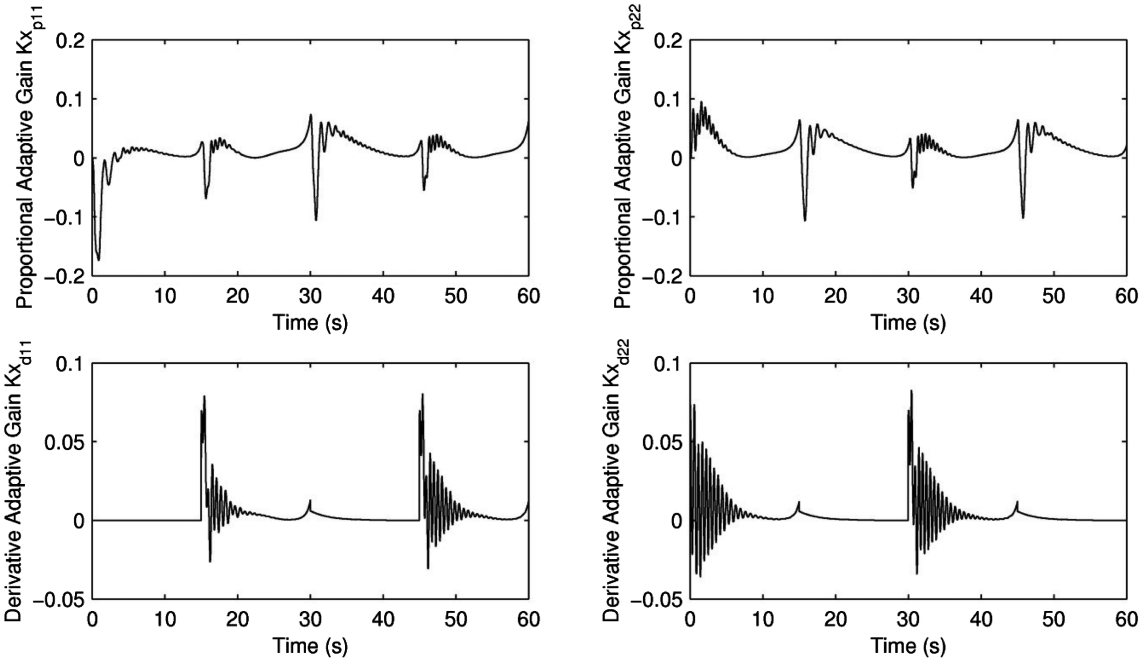

Fig. 17 Adaptation history of the DSAC composite controller gains K_x, uncertain linear joint stiffness manipulator ($k = 200I_2$ N · m).

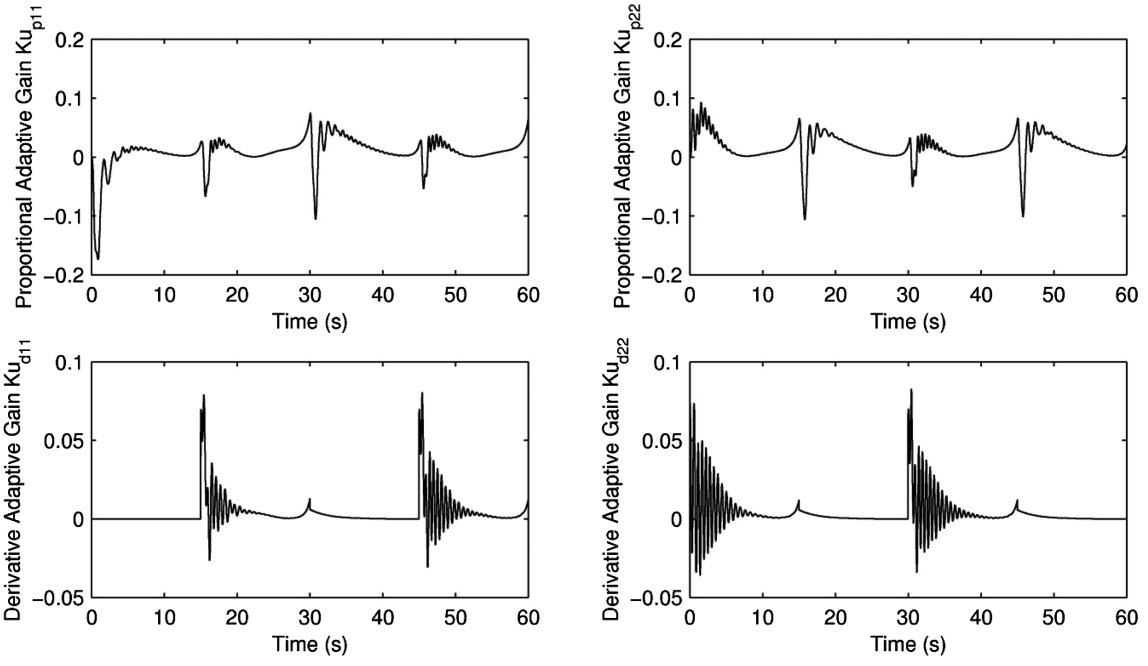

Fig. 18 Adaptation history of the DSAC composite controller gains K_u, uncertain linear joint stiffness manipulator ($k = 200I_2$ N · m).

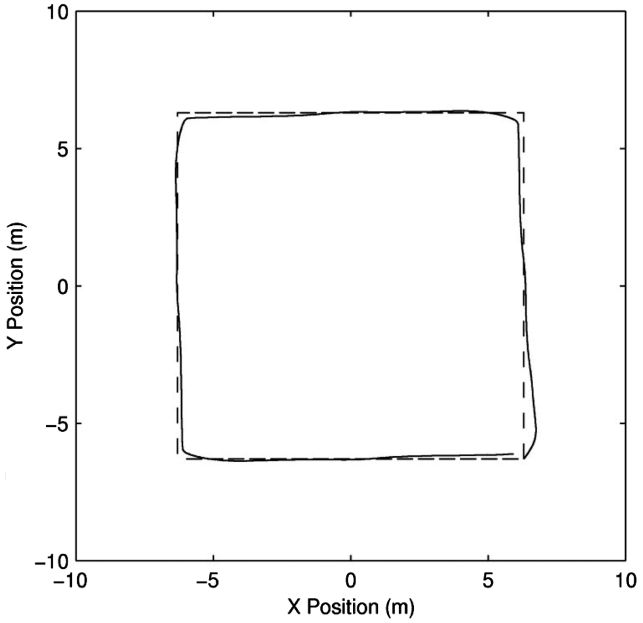

Fig. 19 DMSAC trajectory-tracking results, nonlinear joint stiffness manipulator.

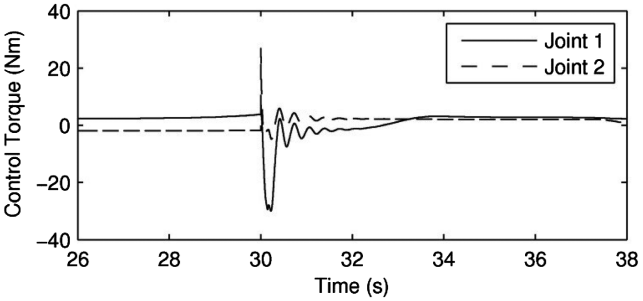

Fig. 20 DMSAC control input torque, nonlinear joint stiffness manipulator.

applied to a nonlinear joint stiffness dynamics model that includes friction torques, nonlinear time-varying joint stiffness matrix, soft-windup effect, and inertial cross-coupling between joint and motor accelerations [13]. For completeness, this model is reported in the Appendix. Again, the controllers were not retuned for this case. Both adaptive control strategies provide a stable closed-loop behavior, yet the trajectory obtained with the DSAC law demonstrates improved tracking results compared to the DMSAC approach, especially along each side of the trajectory, shown in Figs. 19–22. The control inputs for both control strategies are provided in Figs. 20–23, and control gains in Figs. 21 and 24–26.

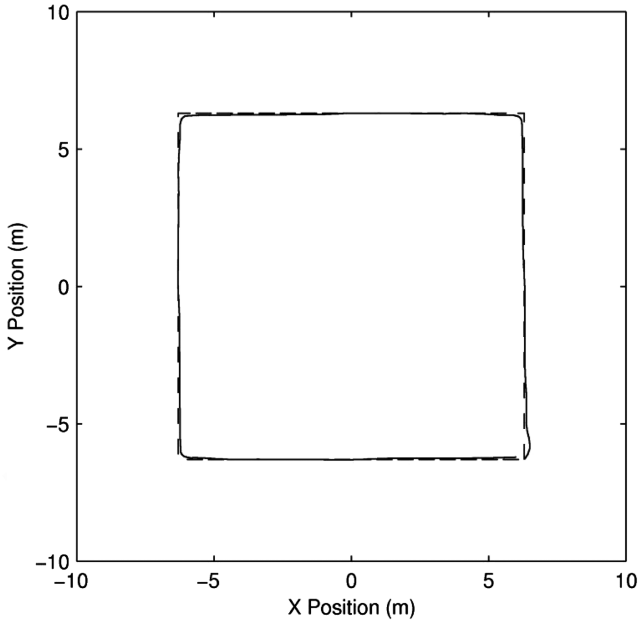

Fig. 22 DSAC trajectory-tracking results, nonlinear joint stiffness manipulator.

Finally, all control torque inputs can be handled by a typical lightweight flexible-joint mechanism (e.g., HFUC-2A, Harmonic Drive AG), as the maximum control torque peak magnitudes obtained are 56.0 and 32.0 N · m for joints 1 and 2 for the DMSAC controller, compared with 98.8 and 56.4 N · m for joints 1 and 2 for the DSAC controller. These peak control efforts occur initially in all simulation cases to increase the Cartesian velocity of the end effector along the y axis from rest to 0.84 m/s. Thereafter, the control torque magnitudes reach maximum levels of 30.5 and 27.4 N · m for joints 1 and 2 for the DMSAC strategy, compared with 39.8 and 26.9 N · m at the third direction change for both joints for the DSAC strategy.

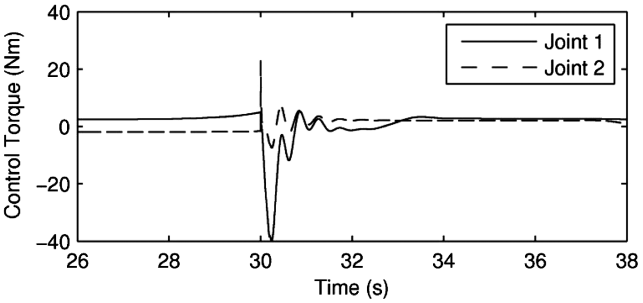

Fig. 23 DSAC control input torque, nonlinear joint stiffness manipulator.

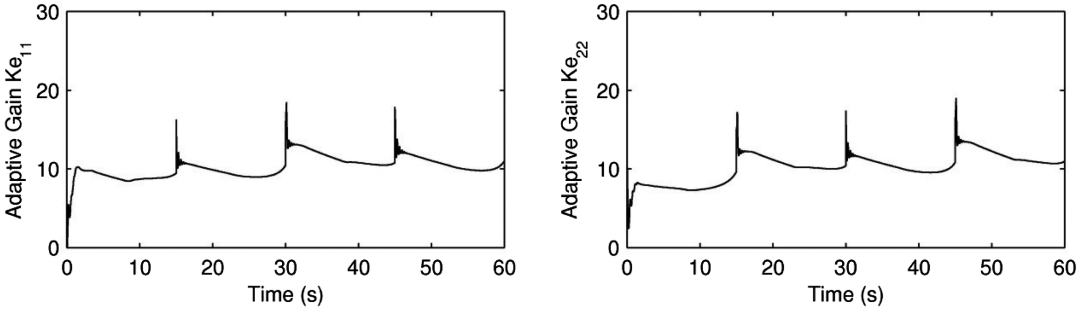

Fig. 21 Adaptation history of the DMSAC composite controller gains K_e, nonlinear joint stiffness manipulator.

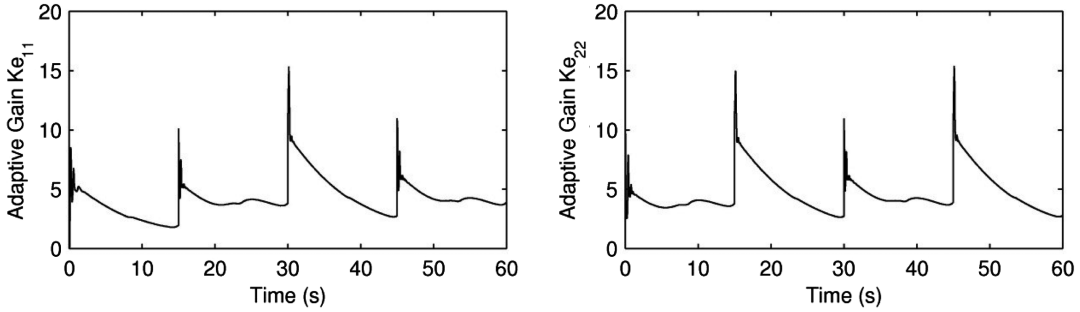

Fig. 24 Adaptation history of the DSAC composite controller gains K_e, nonlinear joint stiffness manipulator.

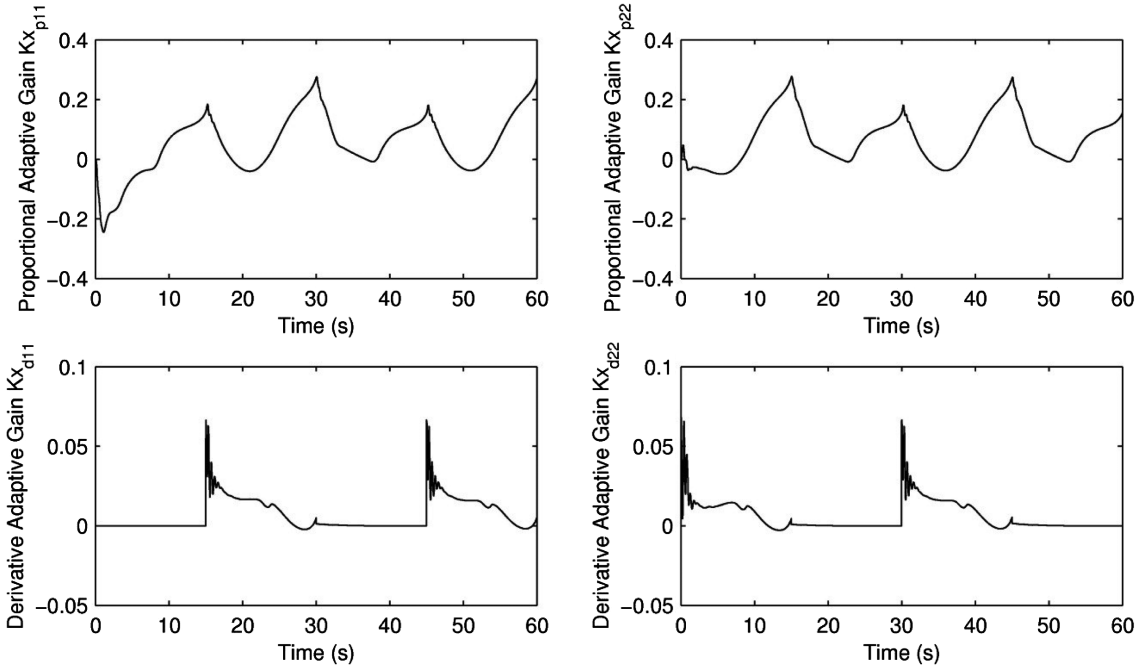

Fig. 25 Adaptation history of the DSAC composite controller gains K_x, nonlinear joint stiffness manipulator.

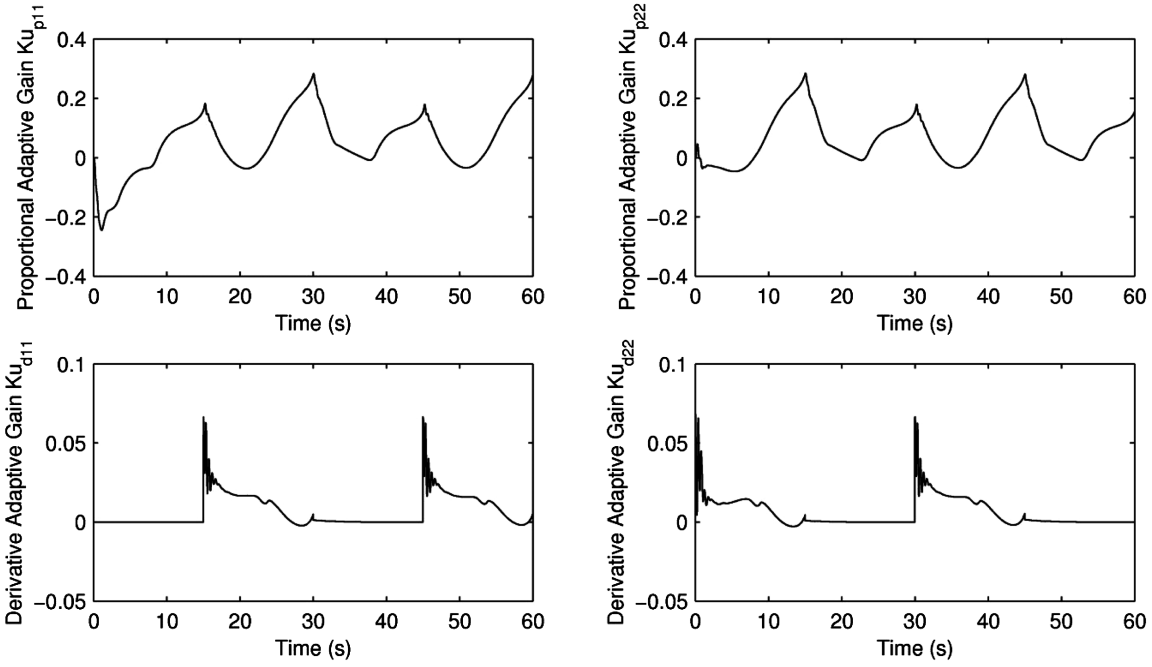

Fig. 26 Adaptation history of the DSAC composite controller gains K_u, nonlinear joint stiffness manipulator.

VII. Conclusions

This paper addressed the problem of adaptive trajectory-tracking control of manipulators that exhibit elastic vibrations in their joints and are subject to parametric uncertainties and modeling errors. It was shown that a flexible-joint manipulator with a scaled-position-plus-velocity feedback signal is almost strictly passive, enabling the use of nonlinear adaptive output feedback control schemes (e.g., simple adaptive control-based methodologies) while guaranteeing the closed-loop stability of the quasi-steady-state model. Two new direct adaptive control schemes designed to stabilize the rigid manipulator dynamics were proposed. The overall stability of the flexible system is guaranteed by invoking Tychonov's theorem. Numerical simulations revealed that both control strategies are efficient at tracking a desired trajectory, regardless of parametric uncertainties and dynamics modeling errors.

While this work aimed at demonstrating the applicability and the performance of the DSAC and DMSAC-based composite control laws for a flexible-joint space manipulator mounted on a stabilized platform, other issues specifically pertaining to space manipulators could be researched as future work, including considering a flexible-joint manipulator mounted on a free-floating platform.

Appendix: Nonlinear Joint Stiffness Dynamics Model

The nonlinear joint stiffness dynamics model developed in [12] and used in this work to validate the robustness of the proposed direct adaptive control laws to dynamics modeling errors is given by

$$M(q)\ddot{q} + S\ddot{q}_m + C(q,\dot{q})\dot{q} + f(\dot{q}) - k(q,q_m)(q_m - q) = 0 \quad \text{(A1)}$$

$$S^T\ddot{q} + J_m\ddot{q}_m + k(q,q_m)(q_m - q) = \tau \quad \text{(A2)}$$

where the nonlinear joint stiffness denoted by $k(q,q_m)(q_m - q)$ is obtained by the following nonlinear cubic function:

$$k(q,q_m)(q_m - q) = a_1\begin{bmatrix}(q_{m1} - q_1)^3\\ (q_{m2} - q_2)^3\end{bmatrix} + a_2(q_m - q) + K_{sw}(q,q_m)(q_m - q) \quad \text{(A3)}$$

where $a_1,\ a_2 \in {}^{2\times 2}$ denotes diagonal positive-definite coefficient matrices defining the nonlinear stiffness curve and where the soft-windup effect, denoted by $K_{sw}(q,q_m) \in \mathbb{R}^{2\times 2}$, decreases the joint stiffness in the region from 0 to 1 N · m. This effect is mathematically modeled a saddle-shaped function as follows:

$$K_{sw}(q,q_m) = -k_{sw}\begin{bmatrix}e^{-a_{sw}(q_{m1}-q_1)^2} & 0\\ 0 & e^{-a_{sw}(q_{m2}-q_2)^2}\end{bmatrix} \quad \text{(A4)}$$

where $k_{sw} \in \mathbb{R}^{2\times 2}$ and $a_{sw} \in \mathbb{R}$, respectively, denote the diagonal positive-definite matrix and parameter defining the soft-windup function.

In Eq. (A1), $f(\dot{q}) \in \mathbb{R}^2$ denotes the continuous and symmetric friction model given by

$$f(\dot{q}) = \gamma_1[\tanh(\gamma_2\dot{q}) - \tanh(\gamma_3\dot{q})] + \gamma_4\tanh(\gamma_5\dot{q}) + \gamma_6\dot{q} \quad \text{(A5)}$$

where, for $\forall\ i = 1, \ldots, 6, \gamma_i \in$ denotes positive parameters defining the different friction components.

Finally, the strictly upper triangular matrix denoted by $S \in \mathbb{R}^{2\times 2}$ models inertial couplings between motor and link accelerations introduced by the dependency of the second rotor's kinetic energy on the first link's angular velocity.

For the simulations, the parameters specific to this nonlinear model were selected as $a_1 = a_2 = 500I_2$ N · m/rad, $k_{sw} = 10I_2$, $a_{sw} = 3000, \gamma_1 = 0.5, \gamma_2 = 150, \gamma_3 = 50, \gamma_4 = 2, \gamma_5 = 100,$ and $\gamma_6 = 0.5$. The inertial coupling matrix is

$$S = \begin{bmatrix}0 & J_{m2}\\ 0 & 0\end{bmatrix}$$

Acknowledgments

This work was financially supported in part by the J. Y. and E. W. Wong Research Award in Mechanical/Aerospace Engineering from Carleton University, the Canadian Space Agency, the Canadian Armed Forces under the S. B. Lerner Memorial Educational Bursary, and the Natural Sciences and Engineering Research Council of Canada under the Alexander Graham Bell Canada Graduate Scholarship CGS D3-374291-2009. The authors also thank the anonymous reviewers and Associate Editor for their useful comments that helped to significantly improve this paper.

References

[1] Sweet, L. M., and Good, M. C., "Re-Definition of the Robot Motion Control Problem: Effects of Plant Dynamics, Drive System Constraints, and User Requirements," *23rd IEEE Conference on Decision and Control*, IEEE, Piscataway, NJ, Dec. 1984, pp. 724–732.

[2] van Woerkom, P. T. L. M., and Misrab, A. K., "Robotic Manipulators in Space: A Dynamics and Control Perspective," *Acta Astronautica*, Vol. 38, Nos. 4–8, 1996, pp. 411–421. doi:10.1016/0094-5765(96)00018-5

[3] Yoo, S. J., "Actuator Fault Detection and Adaptive Accommodation Control of Flexible-Joint Robots," *IET Control Theory and Applications*, Vol. 6, No. 10, 2012, pp. 1497–1507. doi:10.1049/iet-cta.2011.0508

[4] Chang, Y.-C., and Yen, H.-M., "Design of a Robust Position Feedback Tracking Controller for Flexible-Joint Robots," *IET Control Theory and Applications*, Vol. 5, No. 2, 2011, pp. 351–363. doi:10.1049/iet-cta.2010.0166

[5] Kostarigka, A. K., Doulgeri, Z., and Rovithakis, G. A., "Prescribed Performance Tracking for Flexible Joint Robots with Unknown Dynamics and Elasticity," *IEEE International Conference on Robotics and Automation*, IEEE, Piscataway, NJ, May 2012, pp. 5365–5370.

[6] Chatlatanagulchai, W., and Meckl, P. H., "Model-Independent Control of a Flexible-Joint Robot Manipulator," *Journal of Dynamical Systems, Measurements, and Control*, Vol. 131, No. 4, 2009, Paper 041003. doi:10.1115/1.3117185

[7] Lee, J. Y., Yeon, J. S., Park, J. H., and Lee, S., "Robust Back-Stepping Control for Flexible-Joint Robot Manipulators," *IEEE International Conference on Intelligent Robots and Systems*, IEEE, Piscataway, NJ, 2007, pp. 183–188.

[8] Melhem, K., and Wang, W., "Global Output Tracking Control of Flexible Joint Robots via Factorization of the Manipulator Mass Matrix," *IEEE Transaction on Robotics*, Vol. 25, No. 2, 2009, pp. 428–437. doi:10.1109/TRO.2009.2012016

[9] Consolini, L., Gereli, O., Bianco, C. G. L., and Piazzi, A., "Minimum-Time Control of Flexible Joints with Input and Output Constraints," *IEEE International Conference on Robotics and Automation*, IEEE, Piscataway, NJ, 2007, pp. 3811–3816.

[10] Tomei, P., "Tracking Control of Flexible Joint Robots with Uncertain Parameters and Disturbances," *IEEE Transactions on Automatic Control*, Vol. 39, No. 5, 1994, pp. 1067–1072. doi:10.1109/9.284895

[11] Narendra, K. S., and Valavani, L. S., "Direct and Indirect Model Reference Adaptive Control," *Automatica*, Vol. 15, No. 6, 1979, pp. 653–664. doi:10.1016/0005-1098(79)90033-5

[12] Ulrich, S., Sasiadek, J. Z., and Barkana, I., "Modeling and Direct Adaptive Control of a Flexible-Joint Manipulator," *Journal of Guidance, Control, and Dynamics*, Vol. 35, No. 1, 2012, pp. 25–39. doi:10.2514/1.54083

[13] Ulrich, S., and Sasiadek, J. Z., "Direct Fuzzy Adaptive Control of a Manipulator with Elastic Joints," *Journal of Guidance, Control, and Dynamics*, Vol. 36, No. 1, 2013, pp. 311–319. doi: 10.2514/1.57585

[14] Huang, L., Ge, S. S., and Lee, T. H., "Position/Force Control of Uncertain Constrained Flexible Joint Robots," *Mechatronics*, Vol. 16, No. 2, 2006, pp. 111–120. doi:10.1016/j.mechatronics.2005.10.002

[15] Cao, Y., and de Silva, C. W., "Dynamic Modeling and Neural-Network Adaptive Control of a Deployable Manipulator System," *Journal of Guidance, Control, and Dynamics*, Vol. 29, No. 1, 2006, pp. 192–194. doi:10.2514/1.11032

[16] Ulrich, S., "Direct Adaptive Control Methodologies for Flexible-Joint Space Robotic Manipulators with Uncertainties and Modeling Errors," Ph.D. Thesis, Dept. of Mechanical and Aerospace Engineering, Carleton Univ., Ottawa, ON, Canada, Aug. 2012.

[17] Ulrich, S., Sasiadek, J. Z., and Barkana, I., "On a New Class of Direct Adaptive Output Feedback Controllers for Nonlinear Square Systems," *IEEE Conference on Decision and Control*, IEEE, Piscataway, NJ, Dec. 2012, pp. 4139–4144.

[18] Ulrich, S., and Sasiadek, J. Z., "Decentralized Simple Adaptive Control for Nonlinear Systems," *International Journal of Adaptive Control and Signal Processing*, 2013.
doi:10.1002/acs.2446

[19] Barkana, I., "Output Feedback Stabilizability and Passivity in Non-stationary and Nonlinear Systems," *International Journal of Adaptive Control and Signal Processing*, Vol. 24, No. 7, 2010, pp. 568–591.
doi:10.1002/acs.1149

[20] Khalil, H. K., *Nonlinear Systems*, 3rd ed., Prentice–Hall, Upper Saddle River, NJ, 2002, pp. 430–434.

[21] Spong, M. W., "Modeling and Control of Elastic Joint Robots," *Journal of Dynamic Systems, Measurement and Control*, Vol. 109, No. 4, 1987, pp. 310–319.
doi:10.1115/1.3143860

[22] Spong, M. W., Hutchinson, S., and Vidyasagar, M., *Robot Modeling and Control*, Wiley, New York, 2006, p. 85.

[23] Landau, I., "A Survey of Model Reference Adaptive Techniques: Theory and Applications," *Automatica*, Vol. 10, No. 4, 1974, pp. 353–379.
doi:10.1016/0005-1098(74)90064-8

[24] Tao, G., *Adaptive Control System and Analysis, Adaptive and Learning Systems for Signal Processing, Communications and Control Series*, Wiley, Hoboken, NJ, 2003, pp. 149–154.

[25] Kokotovic, P., Khalil, H. K., and O'Reilly, J., *Singular Perturbation Methods in Control: Analysis and Design*, Classics in Applied Mathematics Series, SIAM, Philadelphia, 1999, pp. 1–45.

[26] Spong, M. W., "Adaptive Control of Flexible Joint Manipulators: Comments on Two Papers," *Automatica*, Vol. 31, No. 4, 1995, pp. 585–590.
doi:10.1016/0005-1098(95)98487-Q

[27] Ott, C., *Cartesian Impedance Control of Redundant and Flexible-Joint Robots*, Springer Tracts in Advanced Robotics, Springer, Berlin, Vol. 49, 2008, pp.65–75.

[28] Kaufman, H., Barkana, I., and Sobel, K., *Direct Adaptive Control Algorithms: Theory and Applications*, 2nd ed., Communications and Control Engineering Series, Springer, New York, 1997, pp. 42–45, 55.

[29] Fradkov, A. L., "Synthesis of Adaptive System of Stabilization Linear Dynamic Plants," *Automation and Remote Control*, Vol. 35, No. 12, 1974, pp. 1960–1966.

[30] Fradkov, A. L., "Quadratic Lyapunov Functions in the Adaptive Stability Problem of a Linear Dynamic Target," *Siberian Mathematical Journal*, Vol. 17, No. 2, 1976, pp. 436–447.

[31] Barkana, I., and Kaufman, H., "Global Stability and Performance of a Simplified Adaptive Algorithm," *International Journal of Control*, Vol. 42, No. 6, 1985, pp. 1491–1505.
doi:10.1080/00207178508933440

[32] Ulrich, S., and de Lafontaine, J., "Autonomous Atmospheric Entry on Mars: Performance Improvement Using a Novel Adaptive Control Algorithm," *Journal of the Astronautical Sciences*, Vol. 55, No. 4, 2007, pp. 431–449.
doi:10.1007/BF03256534

[33] Barkana, I., "Defending the Beauty of the Invariance Principle," *International Journal of Control*, Vol. 87, No. 1, 2014, pp. 186–206.
doi:10.1080/00207179.2013.826385

[34] LaSalle, J., "Stability of Non-Autonomous Systems," *Nonlinear Analysis: Theory, Methods, and Applications*, Vol. 1, No. 1, 1981, pp. 83–90.
doi:10.1016/0362-546X(76)90011-0

[35] Ioannou, P. A., and Kokotovic, P., *Adaptive Systems with Reduced Models*, Springer–Verlag, New York, 1983.

[36] Readman, M. C., *Flexible Joint Robots*, Mechatronics Series, CRC Press, Boca Raton, FL, 1994, p. 4.

[37] Banerjee, A. K., and Singhose, W., "Command Shaping in Tracking Control of a Two-Link Flexible Robot," *Journal of Guidance, Control, and Dynamics*, Vol. 21, No. 6, 1998, pp. 1012–1015.
doi:10.2514/2.4343

[38] Green, A., and Sasiadek, J. Z., "Adaptive Control of a Flexible Robot Using Fuzzy Logic," *Journal of Guidance, Control, and Dynamics*, Vol. 28, No. 1, 2005, pp. 36–42.
doi:10.2514/1.6376

[39] Ulrich, S., and Sasiadek, J. Z., "Control Strategies for Flexible Joint Manipulators," *AIAA Guidance, Navigation, and Control Conference*, AIAA Paper 2011-6297, Aug. 2011.